THE FASEB JOURNAL • RESEARCH • www.fasebj.org

Mettl17, a regulator of mitochondrial ribosomal RNA modifications, is required for the translation of mitochondrial coding genes

Zhennan Shi,[*,1] Siyuan Xu,[*,1] Shenghui Xing,[*] Ke Yao,[†] Lei Zhang,[‡] Luxi Xue,[*] Peng Zhou,[§] Ming Wang,[§] Guoquan Yan,[‡] Pengyuan Yang,[‡] Jing Liu,[‖] Zeping Hu,[†,2] and Fei Lan[*,3]

[*]Key Laboratory of Epigenetics and Metabolism, Ministry of Science and Technology, Institutes of Biomedical Sciences, and Key Laboratory of Carcinogenesis and Cancer Invasion, Ministry of Education, Liver Cancer Institute, Zhongshan Hospital, Fudan University, Shanghai, China; [†]School of Pharmaceutical Sciences, Tsinghua University, Beijing, China; [‡]Institutes of Biomedical Sciences and Department of Systems Biology for Medicine, Basic Medical College, Fudan University, Shanghai, China; [§]Key Laboratory of RNA Biology, Institute of Biophysics, Chinese Academy of Sciences, Beijing, China; and [‖]Key Laboratory of Regenerative Biology, South China Institute for Stem Cell Biology and Regenerative Medicine, Guangzhou Institutes of Biomedicine and Health, Chinese Academy of Sciences, Guangzhou, China

ABSTRACT: Embryonic stem cells (ESCs) are pluripotent stem cells with the ability to self-renew and to differentiate into any cell types of the 3 germ layers. Recent studies have demonstrated that there is a strong connection between mitochondrial function and pluripotency. Here, we report that methyltransferase like (Mettl) 17, identified from the clustered regularly interspaced short palindromic repeats knockout screen, is required for proper differentiation of mouse embryonic stem cells (mESCs). Mettl17 is located in mitochondria through its N-terminal targeting sequence and specifically interacts with 12S mitochondrial ribosomal RNA (mt-rRNA) as well as small subunits of mitochondrial ribosome (MSSUs). Loss of Mettl17 affects the stability of both 12S mt-rRNA and its associated proteins of MSSUs. We further showed that Mettl17 is an *S*-adenosyl methionine (SAM)-binding protein and regulates mitochondrial ribosome function in a SAM-binding–dependent manner. Loss of Mettl17 leads to around 70% reduction of m4C840 and 50% reduction of m5C842 of 12S mt-rRNA, revealing the first regulator of the m4C840 and indicating a crosstalk between the 2 nearby modifications. The defects of mitochondrial ribosome caused by deletion of Mettl17 lead to the impaired translation of mitochondrial protein-coding genes, resulting in significant changes in mitochondrial oxidative phosphorylation and cellular metabolome, which are important for mESC pluripotency.—Shi, Z., Xu, S., Xing, S., Yao, K., Zhang, L., Xue, L., Zhou, P., Wang, M., Yan, G., Yang, P., Liu, J., Hu, Z., Lan, F. Mettl17, a regulator of mitochondrial ribosomal RNA modifications, is required for the translation of mitochondrial coding genes. FASEB J. 33, 13040–13050 (2019). www.fasebj.org

KEY WORDS: rRNA modification · 12S rRNA · oxidative phosphorylation

Embryonic stem cells (ESCs) belong to a distinguished type of cells that are immortal, self renewing, and pluripotent. They can differentiate into any type of the 3 germ layer cells (1). To maintain the ability of self renewal and fast cycling, the metabolism of ESC is heavily dependent on glycolysis, which provides cofactors and building materials to biosynthesis and supports cell proliferation of ESCs (2). Upon differentiation, significant metabolic programming takes place, turning glycolysis to mitochondrial oxidative phosphorylation (oxphos) (3). In order to meet

ABBREVIATIONS: ChIRP, comprehensive identification of RNA-binding protein; Cox, cyclooxygenase; CRISPR, clustered regularly interspaced short palindromic repeats; EpiLC, epiblast-like cell; ESC, embryonic stem cell; ETC, electron transport chain; FACS, fluorescence activated cell sorting; GFP, green fluorescent protein; GSH, γ-glutamyl-cysteinyl-glycine; GST, glutathione *S*-transferase; HA, hemagglutinin; KO, knockout; LC-MS/MS, liquid chromatography-tandem mass spectrometry; Med, mediator complex; mESC, mouse ESC; METTL, methyltransferase like; MLSU, large subunit of mitochondrial ribosome; MRM, multiple reaction monitoring; Mrp, mitochondrial ribosomal protein; MSSU, small subunit of mitochondrial ribosome; mt-rRNA, mitochondrial ribosomal RNA; MTS, mitochondria-targeting sequence; Nsun4, NOP2/Sun RNA methyltransferase 4; OCR, oxygen consumption rate; oxphos, oxidative phosphorylation; qPCR, quantitative PCR; qRT-PCR, quantitative RT-PCR; RIP, RNA immunoprecipitation; SAM, *S*-adenosyl methionine; sgRNA, single guide RNA; TCA, tricarboxylic acid cycle; TFB1M, transcription factor B1, mitochondrial

[1] These authors contributed equally to this work.
[2] Correspondence: School of Pharmaceutical Sciences, Tsinghua University, Beijing 100084, China. E-mail: zeping_hu@tsinghua.edu.cn
[3] Correspondence: Liver Cancer Institute, Zhongshan Hospital, Fudan University, Room 504, Mingdao Building, 131 Dongan Rd., Xuhui District, Shanghai 200032, China. E-mail: fei_lan@fudan.edu.cn

doi: 10.1096/fj.201901331R
This article includes supplemental data. Please visit *http://www.fasebj.org* to obtain this information.

 0892-6638/19/0033-13040 © FASEB

the increased demand for oxphos, which is more efficient for energy production, series changes of mitochondria [including numbers, structure, and electron transport chain (ETC) density] couple with the differentiation process (4).

Originated from bacteria, mitochondria are highly specialized and dynamic organelles that play fundamental roles in eukaryotic cells. Although most mitochondrial proteins are encoded by the nuclear genome, mitochondria still keep a 16.6 kb circular genome [mitochondrial (mt)DNA] composed of 13 protein-coding genes that encode components of ETC complexes, and it also has 22 mitochondrially-encoded transfer RNAs (mt-tRNAs) and 2 mitochondrial ribosomal RNA (mt-rRNA) (12S and 16S). The 12S and 16S mt-rRNAs are required for the assembly of small subunit of mitochondrial ribosome (MSSU) and large subunit of mitochondrial ribosome (MLSU), respectively. The translation of 13 protein-coding genes takes place in mitochondria by dedicated mitochondrial ribosomes. Following endonucleolytic cleavage of newly transcribed polycistronic mitochondrial RNA transcripts, mitochondrial ribosomal RNAs (mt-rRNAs) must undergo a series of nucleotide modifications. These modifications are essential for mammalian mitochondrial ribosomal biogenesis. There are 5 known modified residues in mouse 12S mt-rRNA and 4 in 16S mt-rRNA (5, 6). For 12S mt-rRNA, transcription factor B1, mitochondrial (Tfb1m) is responsible for nucleobase dimethylation of adenines A937 and A938 (Mus musculus numbering) (7), whereas NOP2/Sun RNA methyltransferase 4 (Nsun4) mediates 5-methylcytidine at position 842 (8, 9). However, regulators for the other 2 modified residues, m4C840 and m5U425, have not been reported. For 16S rRNA, a group of 2′-*O*-ribose methyltransferases [multiple reaction monitoring (MRM) 1, MRM2/FtsJ2, and MRM3/RNMTL1] have been shown to be involved in the modification of Gm1160, Um1387, and Gm1389, respectively, 3 nt positions of the peptidyl transferase center of 16S mt-rRNA (10, 11). In addition, pseudouridine synthase RPUSD4 has been identified as an enzyme that provide the Psi1416 modification of 16S mt-rRNA (12).

Methyltransferase like (METTL) family proteins are broadly involved in mRNA stability and translation efficiency. For instance, a METTL3-METTL14 complex, the N^6-adenosine-methyltransferase, modulates mRNA stability and protein translation efficiency partially through RNA m6A reader proteins, YTH domain family, member (YTHDF)2 and YTHDF1 (13–15). METTL10, METTL13, and METTL21B are reported to be the methyltransferases for the K318, K55, and K165 site of elongation factor 1-α (eEF1A), which is a crucial factor promoting the GTP-dependent binding of aminoacyl-tRNA to the ribosomal A-site (16–19). METTL1, METTL2, and METTL6 are reported to be the methyltransferases for specific tRNAs (20, 21). Interestingly, certain METTL family proteins, such as METTL12 and METTL20, localize to mitochondria. METTL12 is reported to methylate the K395 site of citrate synthase in mitochondria and regulates citrate synthase activity and cellular metabolism status (22). METTL20 methylate electron transfer flavoprotein β, inhibiting electron transfer flavoprotein β's ability to mediate electron transfer from acyl-CoA dehydrogenases (23). Due to these important regulatory roles, alterations in METTL proteins have been associated with diseases and development (18, 24, 25). Among the METTL family proteins, METTL17 was reported to be a mitochondrial protein associated with a mitoribosome interacting GTPase, C4orf14 (26). Importantly, its ablation could lead to significantly impaired translation of mitochondrial protein-coding genes (27). However, the underlying mechanism remains unclear.

In order to identify unknown regulators involved in the differentiation process of mouse ESCs, we performed a focused clustered regularly interspaced short palindromic repeats (CRISPR) knockout (KO) screen using a green fluorescent protein (GFP) reporter cell in which the GFP expression is driven by the distal enhancer of octamer-binding transcription factor 4 (*Oct4*). The library contains single guide RNAs (sgRNAs) targeting a total of 850 factors, including RNA-binding factors, methyl and acetyl modifiers, and chromatin regulators. Among several potential hits, we focused on Mettl17. The Mettl17 KO mouse ESCs (mESCs) showed delayed differentiation due to compromised mitochondrial oxphos. Our mechanistic study revealed that Mettl17 localized in mitochondria, which is mediated by an N-terminal mitochondria-targeting sequence (MTS; 1–28 aa), and was associated with protein components of MSSUs and 12S mt-rRNA. Loss of Mettl17 led to failures in the full establishment of m4C840 and m5C842 of 12S mt-rRNA, severely compromised integrity of MSSUs, and mitochondrial protein translation. In addition, we also demonstrated that the *S*-adenosyl methionine (SAM)-binding ability of Mettl17 is required for its mitochondrial function.

MATERIALS AND METHODS

Antibodies, constructs, and databases

Antibodies used in this study are listed in Supplemental Table S2. Overexpression of *Mettl17* (NM_001029990.1) wild type and mutants were based on pPB-CAG-ires-puro system. MTS was predicted by Mitoprot program (*https://ihg.gsf.de/ihg/mitoprot.html*). The glutathione *S*-transferase (GST)-tagged recombinant proteins were based on pGEX4T-1 system. Mitocarta is an inventory of mammalian mitochondrial genes (*https://www.broadinstitute.org/scientific-community/science/programs/metabolic-disease-program/publications/mitocarta/mitocarta-in-0*).

Cell culture and cell differentiation

Naive mESCs were cultured in N2B27 medium with 2i 0.4 μM PD0325901 from Stemgent (Cambridge, MA, USA); 3 μM CHIR99021 from Amsbio (Abingdon, United Kingdom) and leukemia inhibitory factor (LIF, 1000 U/ml; MilliporeSigma, Burlington, MA, USA) in feeder-free culture dishes precoated with gelatin (MilliporeSigma). Naive mESCs were differentiated into epiblast-like cells (EpiLCs) as previously described (28). Briefly, 1 million mESCs were plated on 10 cm diameter culture dish coated with 16.7 mg/ml fibronectin (MilliporeSigma) and grown in N2B27 medium supplemented with 1% KSR (Thermo Fisher Scientific, Waltham, MA, USA), fibroblast growth factor-basic (bFGF, 12 ng/ml; MilliporeSigma), and Activin A

(20 ng/ml; PeproTech, Rocky Hill, NJ, USA) for 2 d. To induce differentiation from naive ESCs with retinoic acid, 2i and LIF were removed, and retinoic acid (MilliporeSigma) was added at a concentration of 1 μM for indicated days.

Immunofluorescence

Cells were seeded in 24-well plates at a density of 20,000 cells/well 1 d before immunofluorescence examination. To label mitochondria, MitoTracker (250 nM; Thermo Fisher Scientific) was added to medium for 30 min. Through standard fixation, permeabilization, and antibody incubation procedures, confocal imaging was then processed by Leica TCS SP8 System (Leica Microsystems, Buffalo Grove, IL, USA).

Generation of Mettl17 KO cell lines

CRISPR-Cas9 targeting system was used as previously described by Shalem *et al.* (29). The guide RNA sequences are *Mettl17* KO1: 5′-CCGACATTTACCTGTAGAGC-3′ and *Mettl17* KO2: 5′-AGCAAAACCACCGTCCAATC-3′, targeting the exon 3 and 5, respectively (National Center for Biotechnology Information, Bethesda, MD, USA; *Mettl17* reference sequence NM_001029990.1).

CRISPR screening

The full gene list of the CRISPR KO library can be found in Supplemental Table S3. The gRNAs were designed according to a published method by Shalem *et al.* (29), and 100 nontargeting control sgRNAs were also included. The 5200 oligos of the library were synthesized and provided by PicoHelix (Shanghai, China). The primers for CRISPR library construction and sgRNA Illumina Sequencing Library (San Diego, CA, USA) can be found in Supplemental Table S1.

For the screening, cells were seeded, infected, and selected as previously described for the genome-wide screening. After EpiLC induction, 20 million cells were harvested and prepared for GFP fluorescence activated cell sorting (FACS). A total of 2 million GFP low cells and 2 million GFP high cells were collected by FACS, respectively. The genomic DNA of the sorted cells was extracted by Qiagen DNeasy Kit (Qiagen, Germantown, MD, USA). The sgRNA Illumina Sequencing Library was constructed after 2 rounds of PCR amplifications. After sequencing, the data were analyzed according to the Model-Based Analysis of Genome-Wide CRISPR-Cas9 Knockout (MAGeCK) pipeline (30).

Mitochondrial isolation and protease K protection assay

Cells were scraped and washed with cold PBS twice and then resuspended with IB buffer [200 mM sucrose, 10 mM Tris-MOPS (pH 7.5), 1 mM EGTA] for 20 min at 4°C. After 50 stokes in a tissue douncer and centrifugation at 800 *g* for 5 min at 4°C, the supernatants were collected. For mitochondrial isolation, the supernatants were then centrifuged at 15,000 *g* for 10 min at 4°C, and the pellets were saved as crude mitochondria. Crude mitochondria were further purified by loading onto sucrose gradients (17, 31, 42, and 50%) for ultracentrifugation. Protease K protection assay was performed as previously described by Silvestri *et al.* (31).

RNA immunoprecipitation

A total of 5 million Mettl17-Flag-hemagglutinin (HA) stable cells were harvested and lyzed in 3 volumes of lysis buffer [50 mM Tris-Cl (pH 7.5), 150 mM NaCl, 0.5 mM DTT, 0.25% NP40 with protease inhibitor] in ice for 15 min. After centrifugation at 14,000 rpm for 15 min at 4°C, the supernatant was used as the input. For each RNA immunoprecipitation (RIP) reaction, 5 million cells and 10 μl HA beads were used. The precipitated RNA samples were extracted by Trizol and reverse transcribed followed by quantitative PCR (qPCR) detection.

Comprehensive identification of RNA-binding proteins

Comprehensive identification of RNA-binding protein (ChIRP) experiments were performed as previously described by Chu *et al.* (32). We designed 3 evenly distributed biotinylated probes for 12S rRNA. A total of 10 million cells were used for each reaction, and 3 targeting probes for 12S rRNA can be found in Supplemental Table S1.

Sucrose gradient sedimentation

Sucrose gradient sedimentation was performed as previously described by Antonicka *et al.* (33) with minor modification. For each sample, around 1 mg mitochondria protein lysate was used, and the lysates were loaded on a 12 ml 10–30% continuous sucrose gradient (50 mM Tris-Cl, 100 mM KCl, 10 mM $MgCl_2$) and centrifuged at 32,000 rpm for 4 h in a Beckman SW60-Ti rotor. A total of 15 fractions were collected from the top and used for further analyses (real-time qPCR and Western blot).

Metabolome profiling

A total of 3 million cells were extracted using 1 ml of ice-cold 80% methanol and subjected to 3 rapid freeze-thaw cycles. The cells were then centrifuged at 12,000 rpm for 20 min at 4°C. The supernatant containing aqueous metabolites was evaporated to dryness using a SpeedVac concentrator. Metabolites were reconstituted in 100 μl of 0.03% formic acid in analytical-grade water, vortex mixed, and centrifuged to remove insoluble debris. Thereafter, the supernatant was transferred to an HPLC vial for the metabolomics study as previously described by Huang *et al.* (34) with minor modification. Briefly, targeted metabolite profiling was performed on an AB Sciex Qtrap 6500+ Liquid Chromatography/Triple-Quadrupole Mass Specrometer (Sciex, Framingham, MA, USA) with electrospray ionization source in MRM mode. The injection volume was 10 μl. Separation was achieved on an Acquity UPLC HSS T3 Column (2.1 × 150 mm, 1.8 μm) using a Nexera × 2 LC-30A Ultra High Performance Liquid Chromatograph System (Shimadzu Corporation, Kyoto, Japan). The mobile phases employed were 0.03% formic acid in water (A) and 0.03% formic acid in acetonitrile (B). Cell samples were analyzed in a randomized order, and MRM data were acquired using Analyst 1.6.1 software (Sciex). Chromatogram review and peak area integration were performed using MultiQuant software v.2.1 (Sciex). The peak area for each detected metabolite was normalized against the total ion current of all the detected metabolites within that sample to correct any possible variations. The normalized area values were used as variables for statistical data analysis with a Student's *t* test.

In vitro SAM-binding assay

Recombinant proteins of GST-tagged Mettl17-WT and Mettl17-SAM-mut were expressed in the *Escherichia coli* Rosetta strain and purified with glutathione agarose beads (Smart-Lifesciences, Changzhou, China). For each reaction, 50 ml bacterial culture and

20 μl beads were used, the beads with affinity attached recombinant Mettl17 protein were washed 3 times by wash buffer (20 mM Tris-Cl pH 7.4, 300 mM NaCl, 0.1% Triton X-100) and once by HMT buffer (50 mM Tris-Cl pH 8, 50 mM NaCl, 2 mM $MgCl_2$, 0.1% Triton X-100, 1 mM TCEP). Then the protein-bead complexes were incubated with 50 μl HMT buffer supplemented with 2 μCi [^{3}H]-SAM for 2 h in ice, and cleaned by 3 more washes of wash buffer before detection by scintillation counter. The SAM-binding abilities were reflected by the intensities of the radioactivity associated with the protein-bead complex.

Isolation of a defined rRNA fragment

To isolate the corresponding fragments of 12S rRNA and 16S rRNA containing known modified residues, we refer to the method as previously described by Ma H *et al*. (35) with minor modifications. Briefly, we used 200 pmol of biotin-tagged synthetic oligodeoxynucleotide probe and 200 μg of total RNA or 40 μg mitochondrial RNA for one experiment and the sequences of the probes are listed in Supplemental Table S1. The duplex of the probe and corresponding RNA fragment is purified with streptavidin C1 beads after digestion with mung bean nuclease (New England Biolabs, Ipswich, MA, USA) and RNaseA to eliminate the single-stranded RNA and DNA contaminants.

Liquid chromatography-tandem mass spectrometry

One hundred nanograms of total RNA or purified rRNA fragments was digested by nuclease P1(1U; Wako Pure Chemicals, Tokyo, Japan) in 25 μl of buffer containing 25 mM NaCl and 2.5 mM of ZnCl at 42°C for 2 h, which was followed by addition of NH_4HCO_3 (1 M, 3 μl) and alkaline phosphatase (1U, MilliporeSigma) and additional incubation at 37°C for 2 h. Samples were then diluted to 60 μl and filtered (0.22 μm pore size; MilliporeSigma); 5 μl of solution was loaded into liquid chromatography-tandem mass spectrometry (LC-MS/MS) (Agilent 6410 QQQ Triple-Quadrupole Mass Spectrometer; Santa Clara, CA, USA).

RESULTS

Identification of Mettl17 as a regulator of mESC pluripotency from a CRISPR KO screen

In order to understand the roles of the epigenetics and related factors in the regulation of mESC pluripotency. We constructed a library targeting 850 epigenetics related genes (Supplemental Table S3), with 6 sgRNAs for each gene. We used a well-established $GFP^{DE\ Oct4}$ mES reporter cell line, in which the GFP expression is controlled by the distal enhancer of Oct4 and reflects the pluripotent state (Supplemental Fig. S1*A*). The cells infected by the library were initially cultured in the 2i condition, and then induced to EpiLCs (Supplemental Fig. S1*B*). We collected the GFP high and GFP low populations and sequenced the sgRNAs in the 2 populations. Bioinformatic analysis yielded 43 differentially abundant hits with high confidence (Supplemental Fig. S1*C, D*). The hits covered several previously reported genes, such as *Mettl3*, *Mettl14*, coactivator-associated arginine methyltransferase 1 (*Carm1*), mediator complex subunit (Med)24, *Med6*, and PR/SET domain 14 (*Prdm14*) (36–39), demonstrating the robustness of our screening procedure.

Importantly, we also identified several previously unreported factors. Five of them were later validated including *Mettl17*, SWI/SNF related, matrix associated, actin-dependent regulator of chromatin, subfamily A, member 5 (*Smarca5*), and zinc finger protein 36, C3H type-like 1 (*Zfp36l1*) from the GFP high group and *Med13l* and *Med23* from the GFP low group (Supplemental Fig. S1*E*). Because the Mettl family putative methyltransferases have been shown to play important roles in RNA biology and protein translation–related pathways, we decided to focus on Mettl17 for further investigation.

To further validate the effect of Mettl17 KO on mESC pluripotency, we used 2 *mettl17* KO mESC lines established by 2 independent sgRNAs (**Fig. 1*A***). Using GFP FACS, we found that the GFP intensities of the 2 *Mettl17* KO lines was significantly higher than that of the control cells when differentiated to EpiLC (Fig. 1*B*), consistent with the screening results. The result was also confirmed by expression level analysis of several pluripotent genes measured by qRT-PCR (Fig. 1*C*). Our results thus identified Mettl17 as a previously unreported factor required for mESC to initiate the differentiation process.

Mettl17 is a mitochondrial protein associated with MSSUs

To further characterize the underlining mechanism by which Mettl17 regulates mESC biology, we then look into the subcellular localization of Mettl17 in mESCs. Previous mitochondrial proteome study has shown that Mettl17 is located in mitochondria (40). Because none of the commercial Mettl17 antibodies passed our quality controls for immunofluorescence, we constructed a C terminus Flag and HA-tagged expression construct of Mettl17. Using this stable cell line, we found strong mitochondrial localization of Mettl17-Flag-HA by fluorescence confocal microscopy (Fig. 1*E*), which is independently supported by biochemical isolation of mitochondrial protein extract followed by immunoblotting (Fig. 1*D*). To determine which Mettl17 resides in which mitochondrial compartment, we performed a protease K digestion assay. In the assay, Mettl17 was resistant to proteinase K in both isotonic and hypotonic fractions when the mitochondrial inner membrane remained intact (Fig. 1*F*, lanes 2 and 4), but it was almost completely digested by proteinase K when inner membrane was disrupted (Fig. 1*F*, lane 6). Thus, we concluded that Mettl17 is a mitochondrial inner matrix protein (Fig. 1*F*).

To investigate Mettl17 function in mitochondria, we next sought to characterize its interacting proteins. The mitochondrial protein lysate was enriched with Flag immunoprecipitation and later tested by mass spectrometry (**Fig. 2*A***). Mass spectrometry results were further filtered by the mitochondrial proteome database (MitoCarta) to reduce non-specific contaminations. The Flag immunoprecipitation coupled to mass spectrometry

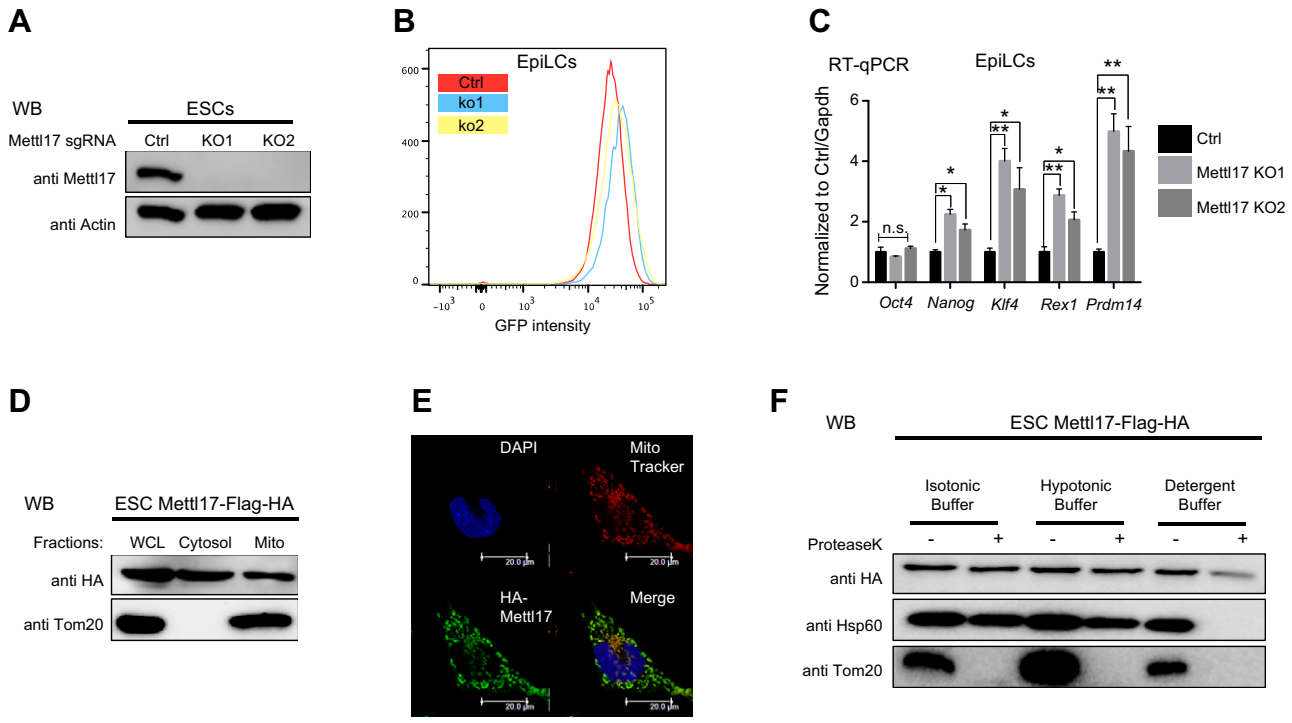

Figure 1. Loss of Mettl17, a mitochondrial protein, resulted in impaired differentiation of mESCs. *A*) Western blot analysis of Mettl17 in the control and 2 Mettl17 KO mES cell lines. *B, C*) GFP FACS (*B*) and the expression analysis of the pluripotent genes by qRT-PCR (*C*) between the control and Mettl17 KO EpiLCs induced from mESCs. Data are presented as means ± SD ($n = 3$) (*C*). $*P < 0.05$, $**P < 0.01$, $***P < 0.001$ (Student's *t* test). *D–F*) Mettl17 is a mitochondrial protein and localizes to the inner mitochondrial membrane matrix. *D*) Western blot analysis of Mettl17 in the indicated cellular fractions, Tom20 is a mitochondrial marker. *E*) Fluorescence confocal analysis of C-term HA-tagged Mettl17 (green), mitotracker labeled mitochondria (red). *F*) Protease K digestion analysis of purified mitochondria from Mettl17-Flag-HA stable cell line of mouse ES.

(IP-MS) identified a total of 150 mitochondrial proteins interacting with Mettl17, with a significant enrichment (24 out of 31) of the components of MSSUs was found (Fig. 2*A*). Interestingly, no components from MLSUs were detected (Fig. 2*A*), suggesting a specific interaction between Mettl17 and MSSUs. In the complex, we also identified C4orf14, a GTPase previously reported to interact with MSSUs and Mettl17 (26). The IP–Western blot showed that Mettl17 interacted with mitochondrial ribosomal protein (Mrp)s15 and Mrps27, 2 components of MSSUs (Fig. 2*B*), but not Mrpl13 and Mrpl44, 2 components of MLSUs (Fig. 2*B*). Because mitochondrial ribosome is a large protein-rRNA complex, we further speculated whether the interaction between Mettl17 and the MSSUs is dependent on the rRNA component. To address this, we treated the Flag immunoprecipitant with RNaseA, and found that the interactions between Mettl17 and Mrps15 or Mrps27 were almost diminished after RNaseA treatment (Fig. 2*B*), indicating a dependence of RNA component, likely the 12S rRNA, the scaffolding RNA of MSSUs.

The findings above suggested that Mettl17 associates with the assembled or partially assembled MSSUs but not individual proteins of MSSUs. To further support this hypothesis, the interaction between Mettl17 and 12S rRNA was readily detectable by both RIP and ChIRP-WB assays (Supplemental Fig. S2*A, C, D*). Taken together, these results demonstrated that Mettl17 is a mitochondrial protein and specifically interacts with MSSUs in an RNA-dependent manner.

Mettl17 is required for MSSU stability, mitoribosome assembly, and protein translation in mitochondria

Given that Mettl17 localizes to mitochondria and specifically interacts with MSSUs, we next wondered whether Mettl17 plays a role in regulating mitochondrial ribosome biogenesis and function. We first examined whether Mettl17 loss affects mitochondria number and gene expression. Using a set of 3 qPCR primers covering 3 loci cross mitochondrial genome, we did not detect any significant changes of mitochondrial DNA copy number (Supplemental Fig. S3*A*), nor did we observe any obvious alteration in the mitochondrial marker protein, Tom20, by immunoblotting, suggesting the mitochondrial biogenesis is largely unaffected. In addition, no significant alterations of the mRNA expression levels of mitochondrial protein-coding genes were detected (**Fig. 3*A***). Thus, we concluded that Mettl17 loss did not lead to global changes of mitochondrial biogenesis or gene transcription.

Although no significant transcription-level changes of the 13 protein-coding genes from mitochondrial genome were detected, we did notice a moderate but significant reduction (~30%) of 12S rRNA in Mettl17 KO cells (Fig. 3*A*). Taken together with the findings above that Mettl17

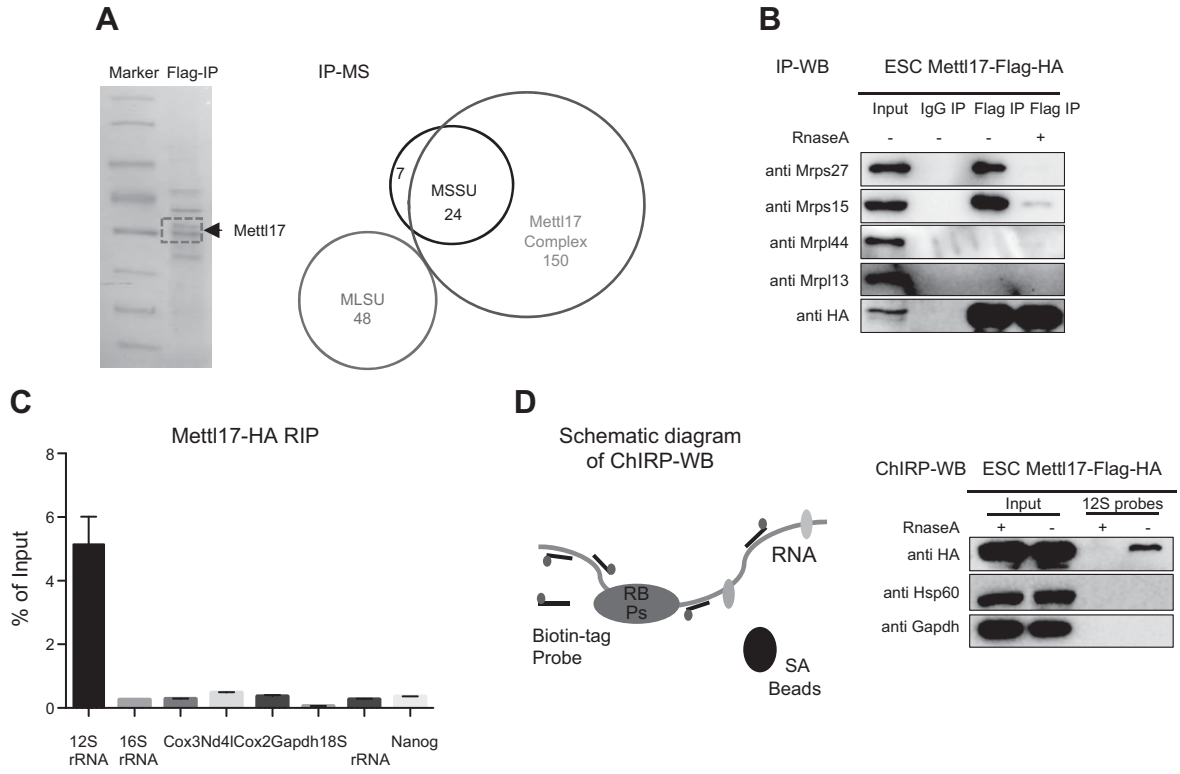

Figure 2. Mettl17 associates with mitochondrial ribosomal small subunit. *A*) Flag affinity purification and MS analysis of Mettl17-Flag-HA protein complex. Left: Flag precipitants were resolved and visualized by coomassie blue staining; Right: Venn diagram analysis of the components of Mettl17 complex and mitochondrial ribosome components. *B*) Western blot analysis of the interaction between Mettl17 and indicated mitochondrial ribosome components under normal and RNaseA treatment. *C*) RIP qPCR analysis of the interactions between Mettl17-Flag-HA and indicated RNA species. *D*) Left: schematic diagram illustration of ChIRP assays; Right: ChIRP-WB analysis of the indicated proteins immunoprecipitated by DNA probes against 12S rRNA.

protein associates with MSSUs (Fig. 2*B, C*), we hypothesized that the specific reduction of 12S mt-rRNA upon loss of Mettl17 is likely due to compromised structural stability but not mitochondrial transcription or splicing defects. Consistent with this hypothesis, we found that some of the MSSU protein components, exemplified by Mrps14 and Mrps15, were significant affected (Fig. 3*B*). However, we did not observe such effect in the 2 large subunit components (Mrpl13 and Mrpl44) examined in our study (Fig. 3*B*). Because mitochondrial ribosomal protein genes are encoded by the nuclear genome and transcript levels of Mrps14 and Mrps15 were not changed in Mettl17 KO cells (Supplemental Fig. S3*B*), such reduction of Mrps14 and Mrps15 proteins may occur at the posttranscriptional step.

To examine the assembly of mitochondrial ribosomes, we detected 12S and 16S mt-rRNAs and their associated ribosome proteins (Mrps14 and Mrpl13) in a 10–30% sucrose gradient, characterizing the distribution of the small (28S) and large (39S) subunits and monosomes (55S) (Supplemental Fig. S3*C*). The control cells showed the same pattern as previously reported by Zhang *et al.* (41). Although the cofractionation ratio of 12S and 16S mt-rRNAs in Mettl17 KO cells was significantly reduced (compared to faction 7–8 and 11–12 in wild-type cells), indicating a major defect in mitoribosome assembly. In addition, the ratio of mRNA encoded by mitochondrial genome was also significantly reduced in 55S mature monosomes (fraction 11–12), which was consistent with the mitoribosome assembly defects. Based on these findings, we speculated that Mettl17 loss cause major failures in mitochondrial ribosome assembly and protein translation. Supporting this, we found that the protein products of randomly selected mitochondrial protein-coding genes, cyclooxygenase (Cox)1 and Cox2, were severely reduced as predicted (Fig. 3*D*).

Mettl17 loss caused significantly altered cellular metabolic state

All of the 13 protein-coding genes encoded by mitochondrial genome are solely translated by mitochondrial ribosome and their protein products are all involved in the formation of ETC complex. We therefore speculated that the oxphos pathway of mitochondria will be affected upon the loss of Mettl17. To test this idea, we then compared the oxygen consumption rate (OCR) of the Mettl17 KO cells with that of the control cells measured by seahorse analyzers and revealed a significant decrease of basal OCR in Mettl17 KO cells (Fig. 3*E*). This was consistent with a previous report of METTL17 as a high-confidence hit from a genome-wide CRISPR death screen essential for oxphos in human myelogenous leukemia K562 cells (27). At the same time, the whole cell metabolite profiling also revealed significant changes in cellular metabolic levels upon Mettl17 deletion (Supplemental Fig. S3*D*). Along

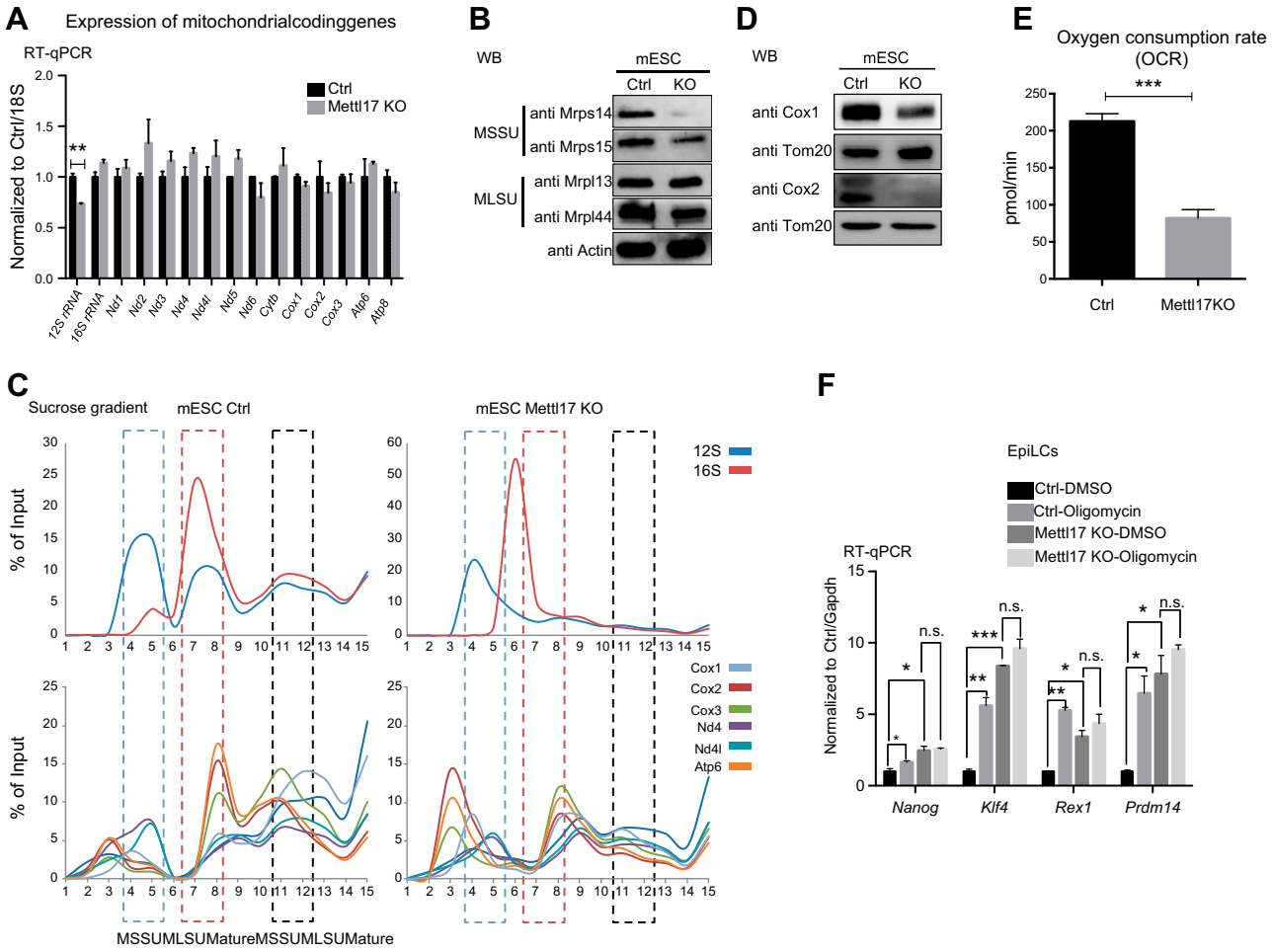

Figure 3. Mettl17 is required for the translation of genes encoded in the mitochondrial genome. *A*) Expression analysis by qRT-PCR of mitochondrial coding genes in the control and Mettl17 KO mESCs. *B*) Western blot analyses of the indicated mitochondrial ribosome components and actin as a loading control in the control and Mettl17 KO mESCs. *C*) Upper panels: the distribution of the mitochondrial ribosome small and large subunits in the indicated sucrose gradient fractions, examined by 12S and 16S rRNA qRT-PCR; Lower panels: the distribution of the mRNAs of the mitochondrial coding genes in the indicated sucrose gradient fractions examined by qRT-PCR. *D*) Western blot analyses of Cox1 and Cox2 protein levels in the control and Mettl17 KO mESCs, and Tom20 was used as control. *E*) OCR of the control and Mettl17 KO cells. *F*) qRT-PCR analyses of the indicated pluripotent genes under the treatments of DMSO or 0.5 μM oligomycin in the control and Mettl17 KO cells. Cells were induced for differentiation to EpiLCs. Data are presented as means ± SD ($n = 3$) (*A*, *E*, *F*). $^*P < 0.05$, $^{**}P < 0.01$, $^{***}P < 0.001$ (Student's *t* test).

with the defect of oxphos, the intermediate metabolites of TCA, citrate, and isocitrate were significantly reduced. Importantly we observed a dramatic increase (33 folds) in the γ-glutamyl-cysteinyl-glycine (GSH)/GSSG ratio (GSSG being the oxidized form of GSH) (Supplemental Fig. S3*D*), which is an indicator for reduced intracellular reactive oxygen species (ROS) level, consistent with the decrease in OCR (Fig. 3*E*). In addition, it was also reported that high GSH levels are required for maintaining stemness (42), which may partly explain mechanistically how Mettl17 KO cells displayed robust stemness.

Moreover, as it is known that mitochondrial oxphos capability is essential for mESC differentiation when cellular metabolism is programed from glycolysis to tricarboxylic acid cycle (TCA), we turned back to the mESC differentiation model described at the beginning and hypothesized that the mESC phenotype was caused by a defect of mitochondrial function, especially oxphos defects, in Mettl17 KO cells. In support of this idea, treatment of oligomycin, an inhibitor of ETC complexes component ATP synthase, had a similar effect to the deletion of Mettl17 and had no additive effect on the differentiation delay phenotype of Mettl17 KO cells (Fig. 3*G*).

The regulation of mitochondrial ribosome function by Mettl17 depends on its SAM binding and mitochondrial localization ability

Mettl17 belongs to the 7-β-strand (7BS) methyltransferase family, with features of a twisted β-sheet structure and conserved sequence motifs. The 7BS methyltransferase family represents the largest methyltransferase class and is able to methylate a wide range of substrates, including RNA, proteins, and lipids (43). After analyzing the primary sequence and secondary structure of Mettl17, we identified a conserved and putative SAM-binding motif

(GxGxG), GSGTG (**Fig. 4*A***). SAM is the cofactor and methyl donor for methyltransferase. Therefore, we sought to test whether Mettl17 is a SAM-binding protein and its dependence on the predicted motif. Using recombinant wild-type and predicted SAM-binding mutant (alanine substitutions in the predicted SAM-binding motif, GSGTG to ASATA) Mettl17 purified from *E. coli*, we performed *in vitro* SAM-binding assay and examined the cobound [^{3}H]-SAM after several washes with radioactivity scintillation counter (Fig. 4*B*). As shown in Fig. 4*B*, the wild-type Mettl17 protein showed strong radioactive signal indicating an ability of SAM binding, whereas the mutant

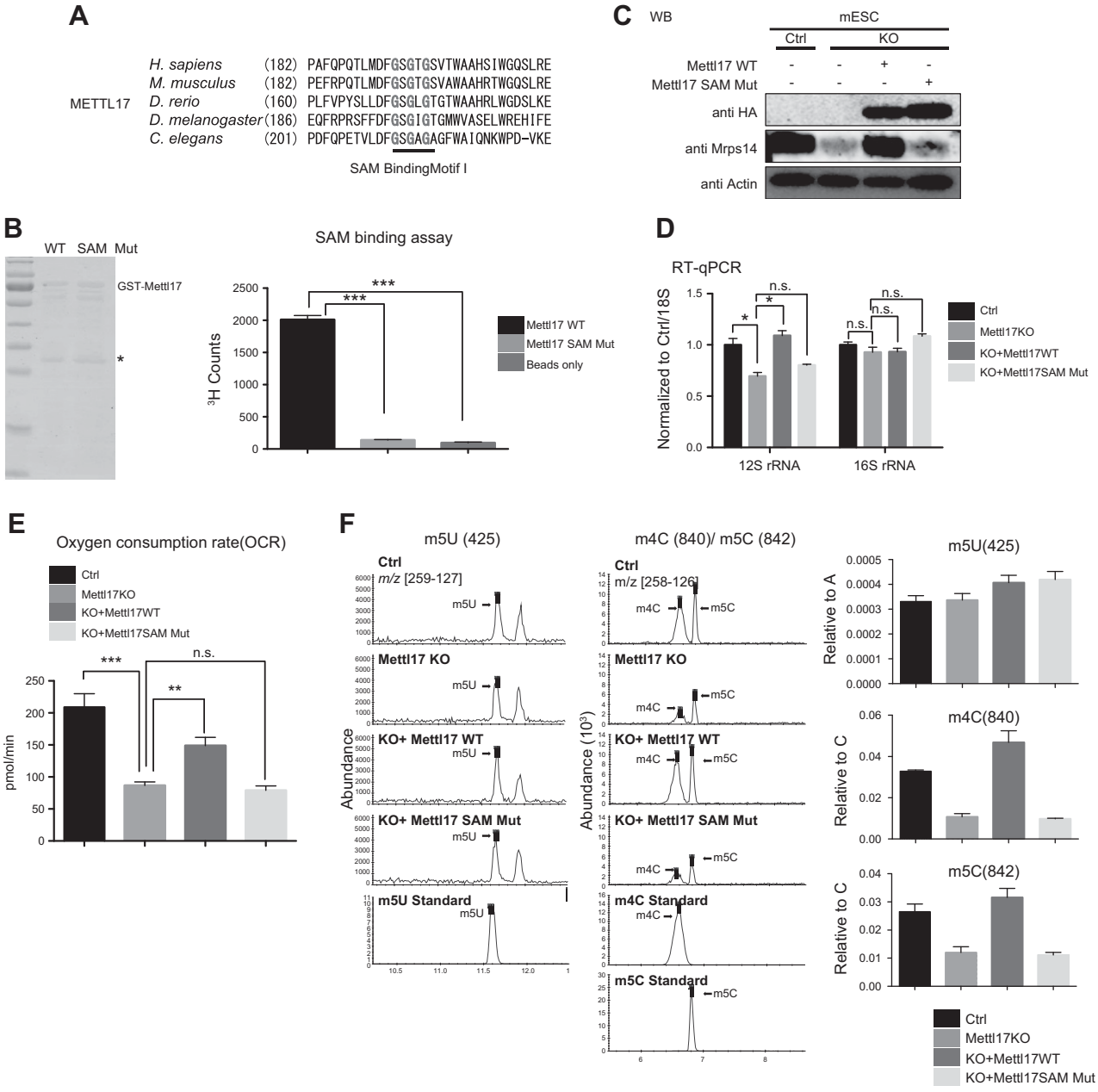

Figure 4. The posttranscriptional modifications of 12S mt-rRNA, m4C and m5C, are regulated by Mettl17 and are correlated with the mitochondrial ribosome function. *A*) Amino acid sequence analysis of the predicted SAM-binding site among Mettl17 homologs in the indicated species. *B*) Left: the purification and coomassie blue staining of the wild-type and point mutant of GST-Mettl17 from *E. coli*. Right: scintillation analysis of the intensities of radioactivity bound by the recombinant wild-type and mutant Mettl17 proteins after incubation with [^{3}H]-SAM *in vitro*, also see Materials and Methods. Asterisk indicates the breakdown product of GST tag. *C–E*) Rescue experiments examining the ability of the wild-type and SAM-binding mutant of Mettl17 to restore MSSU proteins stability (*C*), 12S mt-rRNA (*D*), and OCR (*E*) levels in the Mettl17 KO cells. Data are presented as means ± SD ($n = 3$). *$P < 0.05$, **$P < 0.01$, ***$P < 0.001$ (Student's t test). *F*) Left: LC-MS/MS chromatograms of m5U, m4C, and m5C modifications in the corresponding 12S rRNA fragments purified from mitochondrial RNA. Samples from Ctrl, Mettl17 KO, and the Mettl17 KO mESCs with the wild-type or SAM-binding mutant of Mettl17-Flag-HA rescuing constructs were analyzed; Right: LC-MS/MS quantification of the corresponding modification levels for purified 12S rRNA fragments and normalized against levels of canonical nucleosides.

almost completely lost its SAM-binding ability (Fig. 4*B*). Importantly, we found that the SAM-binding mutant could neither restore the stability of Mrps14 (Fig. 4*C*) nor the level of 12S mt-rRNA (Fig. 4*D*), whereas wild-type Mettl17 could fully restore such defects. In the same time, the reduction of basal OCR could be partially rescued by wild-type Mettl17 but not the SAM-binding mutant (Fig. 4*E*). We also found that the SAM-binding ability is required for the association of Mettl17 with 12S mt-rRNA (Supplemental Fig. S4*E*), suggesting these 2 processes are intrinsically connected.

In addition, we also identified a putative N-terminal MTS by the predictive program Mitoprot (Supplemental Fig. S4*A*) and constructed a rescue cell line with MTS deletion (ΔMTS) (Supplemental Fig. S4*B*). We proved that it is required for mitochondrial localization of Mettl17 by fluorescence confocal (Supplemental Fig. S4*C*). Importantly, the mitochondrial localization mutant (ΔMTS) displayed similar defects as the SAM-binding mutant in rescuing the stability of Mrps14 and Mrps15 and translation of mitochondrial coding protein, Cox1 (Supplemental Fig. S4*D*).

Mettl17 is required for the establishment of m4C and m5C modifications of 12S mt-rRNA

There are 5 reported modifications of 12S mt-rRNA, namely, m5U425, m4C840, m5C842, and $m^6{}_2A937/938$. Based on previous reports, TFB1M is responsible for the $m^6{}_2A$ of A937 and A938 sites, and NSUN4 is responsible for m5C842 (7, 9). To verify whether Mettl17 could be required for the m4C840 or m5U425, we used the well-established method (Supplemental Fig. S4*G*) to quantify the level of RNA modification for a specific rRNA fragment (35) and found that in Mettl17 KO cells, the m4C840 was drastically reduced to around 30% of its level in the control cells, whereas m5U425 did not show any change (Fig. 4*F*). Importantly, such effect was dependent on the SAM-binding ability of Mettl17 (Fig. 4*F*). These raised the possibility of Mettl17 being the yet-to-be identified methyltransferase of m4C840.

Interestingly, in our examination, we also detected a significant but to a lesser extent of reduction of m5C842, likely due to a secondary or crosstalking effect to NSUN4-mediated catalytic event. As a control, we did not find any global effect of Mettl17 loss on m4C and m5C modifications in the total cellular RNA (Supplemental Fig. S4*F*). Importantly, we did not detect any change of the 2 16S rRNA methylations, Gm1160 and Gm1389, in the Mettl17 KO cells (Supplemental Fig. S4*H*). These results indicate that the effects of Mettl17 on the m4C840, and m5C842 of 12S mt-rRNA are rather specific. As we know, the post-transcriptional modifications of 12S mt-rRNA are closely related to the biogenesis and function of mitochondrial ribosome. Cámara *et al.* (8) showed that NSUN4 is required for m5C methylation of 12S rRNA and coordination of mitoribosomal assembly. Metodiev *et al.* (7) showed that $m^6{}_2A$ of 12S mt-rRNA catalyzed by TFB1M is necessary for the stability of MSSUs. Our results showed that the effect of Mettl17 on the stability and function of MSSUs is dependent on its regulation of modifications of 12S mt-rRNA.

In summary, we reported that Mettl17 is a SAM-binding protein and associates with MSSUs. Both Mettl17 protein and its SAM-binding ability are required for the m4C840 and m5C842 of 12S mt-rRNA and mitochondrial ribosome function. Mettl17 loss in mESC led to significantly reduced mitochondrial oxphos and differentiation capability due to a nearly complete loss of mitochondrial translation, which is required to produce essential ETC components.

DISCUSSION

As the powerhouse and center for oxphos, mitochondria are essential for the energy supply and metabolic programing for eukaryotic cells. Mitochondrial dysfunctions are associated with various diseases, including Alzheimer disease, muscular dystrophy, diabetes, and cancers (44). Recent studies in stem cell biology also revealed significant differences in metabolic programs between self-renewal cells and differentiated cells (4). For example, ESCs rely heavily on anaerobic glycolysis, whereas somatic cells mainly use an aerobic metabolism based on oxphos. Upon differentiation, ESCs undergo mitochondrial maturation and bioenergetics transition from glycolysis to oxphos, accompanied with increases of mitochondrial number, respiratory chain complex density, TCA cycle activation, and ATP production (45–47). Along with this line, both stimulation of glycolysis by hypoxia and inhibition of oxphos promote pluripotency (48, 49). Despite numerous changes observed for mitochondrial function and metabolism between ESCs and differentiated cells, the underlying mechanism for such a switch still remains unclear. We speculated that increase of Mettl17 expression upon differentiation is a critical event for the enhancement of mitochondrial function because our data indicate that mitochondrial protein translation is strongly dependent of Metll17 (Fig. 3*D*). However, the regulation of Mettl17 during embryonic development *in vivo* and its effect on differentiation requires a more detailed study in the future.

Here, our findings of Mettl17 in regulating post-transcriptional modifications of 12S mt-rRNA and stability of mitochondrial ribosome, revealed a previously unreported regulatory factor required for mitochondrial ribosomal biogenesis and function. We found that the SAM-binding ability of Mettl17 is important for its mitochondrial function. On this note, together with the previous report that the mutations in SLC25A26, the only known mitochondrial SAM transporter, cause respiratory insufficiency and slowly progressive muscle weakness, pinpointing the importance of mitochondrial SAM supply (50).

In eukaryotic mitochondria, rRNA and tRNA molecules are known to be modified by methylation and other modifications, playing key roles in mitochondrial ribosome biogenesis and efficient and accurate protein translation (51). For instance, TFB1M and NSUN4 are known to mediate $m^6{}_2A937/938$ and m5C842 of 12S mt-rRNA, respectively, and these modification events are important for

mitochondrial ribosome biogenesis and protein translation (7–9). Our results showed that the m4C and m5C of 12S mt-rRNA were reduced by about 50–70% after Mettl17 deletion, and the reduction of m4C is more significant. As we mentioned before, the enzymes that catalyze m5C of 12S mt-rRNA have been identified. We speculate that Mettl17 is the direct enzyme or coregulator for m4C of 12S mt-rRNA. Interestingly, unlike Mettl17, NSUN4 deletion only affects m5C but not m4C (9). One of the possibilities is that the establishment of post-transcriptional modifications on 12S mt-rRNA is sequential and the m4C is established before m5C. To verify this hypothesis, we should set up an *in vitro* methyltransferase enzymatic reaction assay for 12S mt-rRNA and its point mutation counterparts. At this point, we are unclear whether Mettl17 still possesses methyltransferase activity or only utilizes the SAM-binding ability to exert its function. Our findings here certainly call for further investigations on this important question. FJ

ACKNOWLEDGMENTS

The authors thank Dr. Yang Yu (Institute of Biophysics, Chinese Academy of Sciences) and Dr. Ye Tian (Institute of Genetics and Developmental Biology, Chines Academy of Sciences) for instructive discussion. F.L. is funded by the Ministry of Science and Technology of China (2016YFA0101800), Shanghai Municipal Science and Technology Major Project (2017SHZDZX01), and National Science Foundation of China (81773014). Z.H. is supported by grants from Tsinghua University (53332200517) and the National Science and Technology Major Project for Significant New Drugs Development (2017ZX09304015). Z.H. is the recipient of a Bayer Investigator Award. The authors declare no conflicts of interest.

AUTHOR CONTRIBUTIONS

Z. Shi and S. Xu carried out most of the experiments and bioinformatics analyses; S. Xing contributed to the SAM-binding assay and assisted in several experiments; L. Xue carried out part of molecular cloning; L. Zhang, G. Yan, and P. Yang carried out mass spectrometry analyses; J. Liu provided the screening reporter system and constructive insights in ESC biology; P. Zhou and M.W. carried out the GoldCLIP experiment and analyses; K. Yao and Z. Hu carried out the metabolome analyses; and F. Lan conceived the project and cowrote the manuscript with Z. Shi and S. Xu.

REFERENCES

1. Martello, G., and Smith, A. (2014) The nature of embryonic stem cells. *Annu. Rev. Cell Dev. Biol.* **30**, 647–675
2. Kondoh, H., Lleonart, M. E., Nakashima, Y., Yokode, M., Tanaka, M., Bernard, D., Gil, J., and Beach, D. (2007) A high glycolytic flux supports the proliferative potential of murine embryonic stem cells. *Antioxid. Redox Signal.* **9**, 293–299
3. Folmes, C. D., Nelson, T. J., Martinez-Fernandez, A., Arrell, D. K., Lindor, J. Z., Dzeja, P. P., Ikeda, Y., Perez-Terzic, C., and Terzic, A. (2011) Somatic oxidative bioenergetics transitions into pluripotency-dependent glycolysis to facilitate nuclear reprogramming. *Cell Metab.* **14**, 264–271
4. Xu, X., Duan, S., Yi, F., Ocampo, A., Liu, G. H., and Izpisua Belmonte, J. C. (2013) Mitochondrial regulation in pluripotent stem cells. *Cell Metab.* **18**, 325–332
5. Baer, R. J., and Dubin, D. T. (1981) Methylated regions of hamster mitochondrial ribosomal RNA: structural and functional correlates. *Nucleic Acids Res.* **9**, 323–337
6. Van Haute, L., Pearce, S. F., Powell, C. A., D'Souza, A. R., Nicholls, T. J., and Minczuk, M. (2015) Mitochondrial transcript maturation and its disorders. *J. Inherit. Metab. Dis.* **38**, 655–680
7. Metodiev, M. D., Lesko, N., Park, C. B., Cámara, Y., Shi, Y., Wibom, R., Hultenby, K., Gustafsson, C. M., and Larsson, N. G. (2009) Methylation of 12S rRNA is necessary for in vivo stability of the small subunit of the mammalian mitochondrial ribosome. *Cell Metab.* **9**, 386–397
8. Cámara, Y., Asin-Cayuela, J., Park, C. B., Metodiev, M. D., Shi, Y., Ruzzenente, B., Kukat, C., Habermann, B., Wibom, R., Hultenby, K., Franz, T., Erdjument-Bromage, H., Tempst, P., Hallberg, B. M., Gustafsson, C. M., and Larsson, N. G. (2011) MTERF4 regulates translation by targeting the methyltransferase NSUN4 to the mammalian mitochondrial ribosome. *Cell Metab.* **13**, 527–539
9. Metodiev, M. D., Spåhr, H., Loguercio Polosa, P., Meharg, C., Becker, C., Altmueller, J., Habermann, B., Larsson, N. G., and Ruzzenente, B. (2014) NSUN4 is a dual function mitochondrial protein required for both methylation of 12S rRNA and coordination of mitoribosomal assembly. *PLoS Genet.* **10**, e1004110
10. Lee, K. W., and Bogenhagen, D. F. (2014) Assignment of 2′-O-methyltransferases to modification sites on the mammalian mitochondrial large subunit 16 S ribosomal RNA (rRNA). *J. Biol. Chem.* **289**, 24936–24942
11. Rorbach, J., Boesch, P., Gammage, P. A., Nicholls, T. J., Pearce, S. F., Patel, D., Hauser, A., Perocchi, F., and Minczuk, M. (2014) MRM2 and MRM3 are involved in biogenesis of the large subunit of the mitochondrial ribosome. *Mol. Biol. Cell* **25**, 2542–2555
12. Zaganelli, S., Rebelo-Guiomar, P., Maundrell, K., Rozanska, A., Pierredon, S., Powell, C. A., Jourdain, A. A., Hulo, N., Lightowlers, R. N., Chrzanowska-Lightowlers, Z. M., Minczuk, M., and Martinou, J. C. (2017) The pseudouridine synthase RPUSD4 is an essential component of mitochondrial RNA granules. *J. Biol. Chem.* **292**, 4519–4532
13. Wang, X., Lu, Z., Gomez, A., Hon, G. C., Yue, Y., Han, D., Fu, Y., Parisien, M., Dai, Q., Jia, G., Ren, B., Pan, T., and He, C. (2014) N6-methyladenosine-dependent regulation of messenger RNA stability. *Nature* **505**, 117–120
14. Wang, X., Zhao, B. S., Roundtree, I. A., Lu, Z., Han, D., Ma, H., Weng, X., Chen, K., Shi, H., and He, C. (2015) N(6)-methyladenosine modulates messenger RNA translation efficiency. *Cell* **161**, 1388–1399
15. Liu, J., Yue, Y., Han, D., Wang, X., Fu, Y., Zhang, L., Jia, G., Yu, M., Lu, Z., Deng, X., Dai, Q., Chen, W., and He, C. (2014) A METTL3-METTL14 complex mediates mammalian nuclear RNA N6-adenosine methylation. *Nat. Chem. Biol.* **10**, 93–95
16. Shimazu, T., Barjau, J., Sohtome, Y., Sodeoka, M., and Shinkai, Y. (2014) Selenium-based S-adenosylmethionine analog reveals the mammalian seven-beta-strand methyltransferase METTL10 to be an EF1A1 lysine methyltransferase. *PLoS One* **9**, e105394
17. Jakobsson, M. E., Małecki, J. M., Halabelian, L., Nilges, B. S., Pinto, R., Kudithipudi, S., Munk, S., Davydova, E., Zuhairi, F. R., Arrowsmith, C. H., Jeltsch, A., Leidel, S. A., Olsen, J. V., and Falnes, P. Ø. (2018) The dual methyltransferase METTL13 targets N terminus and Lys55 of eEF1A and modulates codon-specific translation rates. *Nat. Commun.* **9**, 3411
18. Liu, S., Hausmann, S., Carlson, S. M., Fuentes, M. E., Francis, J. W., Pillai, R., Lofgren, S. M., Hulea, L., Tandoc, K., Lu, J., Li, A., Nguyen, N. D., Caporicci, M., Kim, M. P., Maitra, A., Wang, H., Wistuba, I. I., Porco, J. A., Jr., Bassik, M. C., Elias, J. E., Song, J., Topisirovic, I., Van Rechem, C., Mazur, P. K., and Gozani, O. (2019) METTL13 methylation of eEF1A increases translational output to promote tumorigenesis. *Cell* **176**, 491–504.e21
19. Malecki, J., Aileni, V. K., Ho, A. Y. Y., Schwarz, J., Moen, A., Sørensen, V., Nilges, B. S., Jakobsson, M. E., Leidel, S. A., and Falnes, P. O. (2017) The novel lysine specific methyltransferase METTL21B affects mRNA translation through inducible and dynamic methylation of Lys-165 in human eukaryotic elongation factor 1 alpha (eEF1A). *Nucleic Acids Res.* **45**, 4370–4389
20. Cartlidge, R. A., Knebel, A., Peggie, M., Alexandrov, A., Phizicky, E. M., and Cohen, P. (2005) The tRNA methylase METTL1 is phosphorylated and inactivated by PKB and RSK in vitro and in cells. *EMBO J.* **24**, 1696–1705

21. Xu, L., Liu, X., Sheng, N., Oo, K. S., Liang, J., Chionh, Y. H., Xu, J., Ye, F., Gao, Y. G., Dedon, P. C., and Fu, X. Y. (2017) Three distinct 3-methylcytidine (m^3C) methyltransferases modify tRNA and mRNA in mice and humans. *J. Biol. Chem.* **292**, 14695–14703
22. Małecki, J., Jakobsson, M. E., Ho, A. Y. Y., Moen, A., Rustan, A. C., and Falnes, P. O. (2017) Uncovering human METTL12 as a mitochondrial methyltransferase that modulates citrate synthase activity through metabolite-sensitive lysine methylation. *J. Biol. Chem.* **292**, 17950–17962
23. Małecki, J., Ho, A. Y., Moen, A., Dahl, H. A., and Falnes, P. O. (2015) Human METTL20 is a mitochondrial lysine methyltransferase that targets the β subunit of electron transfer flavoprotein (ETFβ) and modulates its activity. *J. Biol. Chem.* **290**, 423–434
24. Ma, J. Z., Yang, F., Zhou, C. C., Liu, F., Yuan, J. H., Wang, F., Wang, T. T., Xu, Q. G., Zhou, W. P., and Sun, S. H. (2017) METTL14 suppresses the metastatic potential of hepatocellular carcinoma by modulating N^6 -methyladenosine-dependent primary microRNA processing. *Hepatology* **65**, 529–543
25. Lin, S., Choe, J., Du, P., Triboulet, R., and Gregory, R. I. (2016) The m(6)A methyltransferase METTL3 promotes translation in human cancer cells. *Mol. Cell* **62**, 335–345
26. He, J., Cooper, H. M., Reyes, A., Di Re, M., Kazak, L., Wood, S. R., Mao, C. C., Fearnley, I. M., Walker, J. E., and Holt, I. J. (2012) Human C4orf14 interacts with the mitochondrial nucleoid and is involved in the biogenesis of the small mitochondrial ribosomal subunit. *Nucleic Acids Res.* **40**, 6097–6108
27. Arroyo, J. D., Jourdain, A. A., Calvo, S. E., Ballarano, C. A., Doench, J. G., Root, D. E., and Mootha, V. K. (2016) A genome-wide CRISPR death screen identifies genes essential for oxidative phosphorylation. *Cell Metab.* **24**, 875–885
28. Hayashi, K., Ohta, H., Kurimoto, K., Aramaki, S., and Saitou, M. (2011) Reconstitution of the mouse germ cell specification pathway in culture by pluripotent stem cells. *Cell.* **146**, 519–532
29. Shalem, O., Sanjana, N. E., Hartenian, E., Shi, X., Scott, D. A., Mikkelson, T., Heckl, D., Ebert, B. L., Root, D. E., Doench, J. G., and Zhang, F. (2014) Genome-scale CRISPR-Cas9 knockout screening in human cells. *Science* **343**, 84–87
30. Li, W., Xu, H., Xiao, T., Cong, L., Love, M. I., Zhang, F., Irizarry, R. A., Liu, J. S., Brown, M., and Liu, X. S. (2014) MAGeCK enables robust identification of essential genes from genome-scale CRISPR/Cas9 knockout screens. *Genome Biol.* **15**, 554
31. Silvestri, L., Caputo, V., Bellacchio, E., Atorino, L., Dallapiccola, B., Valente, E. M., and Casari, G. (2005) Mitochondrial import and enzymatic activity of PINK1 mutants associated to recessive parkinsonism. *Hum. Mol. Genet.* **14**, 3477–3492
32. Chu, C., Zhang, Q. C., da Rocha, S. T., Flynn, R. A., Bharadwaj, M., Calabrese, J. M., Magnuson, T., Heard, E., and Chang, H. Y. (2015) Systematic discovery of Xist RNA binding proteins. *Cell* **161**, 404–416
33. Antonicka, H., Sasarman, F., Nishimura, T., Paupe, V., and Shoubridge, E. A. (2013) The mitochondrial RNA-binding protein GRSF1 localizes to RNA granules and is required for post-transcriptional mitochondrial gene expression. *Cell Metab.* **17**, 386–398
34. Huang, F., Ni, M., Chalishazar, M. D., Huffman, K. E., Kim, J., Cai, L., Shi, X., Cai, F., Zacharias, L. G., Ireland, A. S., Li, K., Gu, W., Kaushik, A. K., Liu, X., Gazdar, A. F., Oliver, T. G., Minna, J. D., Hu, Z., and DeBerardinis, R. J. (2018) Inosine monophosphate dehydrogenase dependence in a subset of small cell lung cancers. *Cell Metab.* **28**, 369–382.e5
35. Ma, H., Wang, X., Cai, J., Dai, Q., Natchiar, S.K., Lv, R., Chen, K., Lu, Z., Chen, H., and Shi, Y.G. *et al.* (2019) N(6-)Methyladenosine methyltransferase ZCCHC4 mediates ribosomal RNA methylation. *Nat. Chem. Biol.* **15**, 88–94; erratum: 549
36. Geula, S., Moshitch-Moshkovitz, S., Dominissini, D., Mansour, A. A., Kol, N., Salmon-Divon, M., Hershkovitz, V., Peer, E., Mor, N., Manor, Y. S., Ben-Haim, M. S., Eyal, E., Yunger, S., Pinto, Y., Jaitin, D. A., Viukov, S., Rais, Y., Krupalnik, V., Chomsky, E., Zerbib, M., Maza, I., Rechavi, Y., Massarwa, R., Hanna, S., Amit, I., Levanon, E. Y., Amariglio, N., Stern-Ginossar, N., Novershtern, N., Rechavi, G., and Hanna, J. H. (2015) Stem cells. m6A mRNA methylation facilitates resolution of naïve pluripotency toward differentiation. *Science* **347**, 1002–1006
37. Yamaji, M., Ueda, J., Hayashi, K., Ohta, H., Yabuta, Y., Kurimoto, K., Nakato, R., Yamada, Y., Shirahige, K., and Saitou, M. (2013) PRDM14 ensures naive pluripotency through dual regulation of signaling and epigenetic pathways in mouse embryonic stem cells. *Cell Stem Cell* **12**, 368–382
38. Wu, Q., Bruce, A. W., Jedrusik, A., Ellis, P. D., Andrews, R. M., Langford, C. F., Glover, D. M., and Zernicka-Goetz, M. (2009) CARM1 is required in embryonic stem cells to maintain pluripotency and resist differentiation. *Stem Cells* **27**, 2637–2645
39. Kagey, M. H., Newman, J. J., Bilodeau, S., Zhan, Y., Orlando, D. A., van Berkum, N. L., Ebmeier, C. C., Goossens, J., Rahl, P. B., Levine, S. S., Taatjes, D. J., Dekker, J., and Young, R. A. (2010) Mediator and cohesin connect gene expression and chromatin architecture. *Nature* **467**, 430–435; erratum: 472, 247
40. Pagliarini, D. J., Calvo, S. E., Chang, B., Sheth, S. A., Vafai, S. B., Ong, S. E., Walford, G. A., Sugiana, C., Boneh, A., Chen, W. K., Hill, D. E., Vidal, M., Evans, J. G., Thorburn, D. R., Carr, S. A., and Mootha, V. K. (2008) A mitochondrial protein compendium elucidates complex I disease biology. *Cell* **134**, 112–123
41. Zhang, X., Zuo, X., Yang, B., Li, Z., Xue, Y., Zhou, Y., Huang, J., Zhao, X., Zhou, J., Yan, Y., Zhang, H., Guo, P., Sun, H., Guo, L., Zhang, Y., and Fu, X. D. (2014) MicroRNA directly enhances mitochondrial translation during muscle differentiation. *Cell* **158**, 607–619
42. Jeong, E. M., Yoon, J. H., Lim, J., Shin, J. W., Cho, A. Y., Heo, J., Lee, K. B., Lee, J. H., Lee, W. J., Kim, H. J., Son, Y. H., Lee, S. J., Cho, S. Y., Shin, D. M., Choi, K., and Kim, I. G. (2018) Real-time monitoring of glutathione in living cells reveals that high glutathione levels are required to maintain stem cell function. *Stem Cell Rep.* **10**, 600–614
43. Falnes, P. O., Jakobsson, M. E., Davydova, E., Ho, A., and Małecki, J. (2016) Protein lysine methylation by seven-β-strand methyltransferases. *Biochem. J.* **473**, 1995–2009
44. Pieczenik, S. R., and Neustadt, J. (2007) Mitochondrial dysfunction and molecular pathways of disease. *Exp. Mol. Pathol.* **83**, 84–92
45. Chung, S., Arrell, D. K., Faustino, R. S., Terzic, A., and Dzeja, P. P. (2010) Glycolytic network restructuring integral to the energetics of embryonic stem cell cardiac differentiation. *J. Mol. Cell. Cardiol.* **48**, 725–734
46. Facucho-Oliveira, J. M., Alderson, J., Spikings, E. C., Egginton, S., and St John, J. C. (2007) Mitochondrial DNA replication during differentiation of murine embryonic stem cells. *J. Cell Sci.* **120**, 4025–4034
47. Suhr, S. T., Chang, E. A., Tjong, J., Alcasid, N., Perkins, G. A., Goissis, M. D., Ellisman, M. H., Perez, G. I., and Cibelli, J. B. (2010) Mitochondrial rejuvenation after induced pluripotency. *PLoS One* **5**, e14095
48. Ezashi, T., Das, P., and Roberts, R. M. (2005) Low O2 tensions and the prevention of differentiation of hES cells. *Proc. Natl. Acad. Sci. USA* **102**, 4783–4788
49. Varum, S., Momcilović, O., Castro, C., Ben-Yehudah, A., Ramalho-Santos, J., and Navara, C. S. (2009) Enhancement of human embryonic stem cell pluripotency through inhibition of the mitochondrial respiratory chain. *Stem Cell Res. (Amst.)* **3**, 142–156
50. Menga, A., Palmieri, E. M., Cianciulli, A., Infantino, V., Mazzone, M., Scilimati, A., Palmieri, F., Castegna, A., and Iacobazzi, V. (2017) SLC25A26 overexpression impairs cell function via mtDNA hypermethylation and rewiring of methyl metabolism. *FEBS J.* **284**, 967–984
51. Bohnsack, M. T., and Sloan, K. E. (2018) The mitochondrial epitranscriptome: the roles of RNA modifications in mitochondrial translation and human disease. *Cell. Mol. Life Sci.* **75**, 241–260

Received for publication May 28, 2019.
Accepted for publication August 5, 2019.